Dynamics of Step Bunching in Heteroepitaxial Growth on Vicinal Substrates

Mina Yoon,[1,2] Ho Nyung Lee,[1] Wei Hong,[3] Hans M. Christen,[1] Zhenyu Zhang,[1,2] and Zhigang Suo[3]

[1] *Materials Science and Technology Division, Oak Ridge National Laboratory, Oak Ridge, Tennessee 37831, USA*

[2] *Department of Physics and Astronomy, The University of Tennessee, Knoxville, Tennessee 37996, USA*

[3] *Division of Engineering and Applied Sciences, Harvard University, Cambridge, Massachusetts 02138, USA*

(Received 5 February 2007; published 3 August 2007)

When a heteroepitaxial film is grown on a vicinal substrate, the terrace steps at the growth front may bunch together to relieve strain, resulting in a rough surface. On the other hand, proper manipulation of the growth kinetics may suppress the inherent bunching instability, thus preserving step-flow growth. Here we show that the step dynamics in the early stages of growth can already determine whether the bunching instability is truly suppressed, prior to bunching actually taking place in the unstable regime. We determine the critical film thickness above which steps will bunch and exploit its scaling properties and usefulness for extracting intrinsic energy parameters. Experimental studies of $SrRuO_3$ films grown on vicinal $SrTiO_3$ substrates clearly establish the existence of the critical film thickness in step bunching.

DOI: 10.1103/PhysRevLett.99.055503 PACS numbers: 81.10.Aj, 68.35.Fx, 68.37.Ps, 68.55.−a

Understanding of the morphological evolution in epitaxial growth is an important area of interdisciplinary science [1]. Progress in this area may lead to better control of the fabrication processes of various low-dimensional structures. In particular, considerable effort has been devoted to synthesizing various thin-film materials. These materials may exhibit unique physical properties, which can be exploited to develop new devices. Because the physical properties and device performance of thin films depend critically on the film quality, it remains a challenge to gain precise control of the film morphologies under diverse growth conditions, so that a preferred mode of growth can be selected to meet specific practical needs.

In epitaxial thin films, commonly observed growth modes on a vicinal substrate are step flow, step bunching, and island formation [2,3]. For most device applications, atomically flat films are desired, making step flow the preferred growth mode. Yet, when a heteroepitaxial film is grown on a vicinal substrate, there exists an inherent instability for the steps at the growth front to bunch together to relieve strain, resulting in a rough film [3,4]. Recent studies have shown that proper control of the growth kinetics may suppress the bunching instability, preserving step-flow growth [3,5,6]. This has been demonstrated experimentally [7–9], and certain effective system parameters of fundamental importance have been extracted aided by proper modeling of the growth systems [7,9]. Once such intrinsic system parameters are known, the growth mode under given growth conditions can be predicted, and the film quality can be controlled.

In this Letter, we study theoretically the dynamical evolution of steps at the growth front of an epitaxially strained film on a vicinal substrate. We show that the step dynamics in the early stages of growth can be used to determine whether the bunching instability is truly suppressed, *prior to* step bunching actually taking place in the unstable regime. We also determine the critical film thickness above which step bunching becomes unavoidable and further elucidate the scaling properties of the critical thickness. These scaling relationships allow one to extract intrinsic energy parameters of the system. Preliminary experimental results of $SrRuO_3$ (SRO) films epitaxially grown on vicinal $SrTiO_3$ (STO) substrates confirm qualitatively these predictions, in particular, the existence of the critical film thickness in the bunching regime. The present findings should be instrumental in future experimental efforts to grow smooth films of desired thickness.

We first focus on the step dynamics of an infinite one-dimensional (1D) array of parallel steps as a heteroepitaxial film is grown on a vicinal substrate. During the time of observation, we assume the conservation of step numbers and denote the position of step n at time t by $x_n(t)$. The velocity of the step n (V) is a function of the positions of all of the other steps relative to the step: $r_n = x_{n+j} - x_j$. The 1D translational symmetry of the infinite step array dictates that the function V is the same for every step and independent of the absolute position of each step. Acknowledging this symmetry, the step velocity follows:

$$dx_n/dt = V[(x_{n+1} - x_n), (x_{n+2} - x_n), \ldots, (x_{n-1} - x_n), (x_{n-2} - x_n), \ldots]. \quad (1)$$

We further assume that V does not depend on time explicitly. Under the deposition flux F, the steps flow at the average velocity of FL, where L is the average terrace width. If the terraces are of the same width, the step velocity is expressed as $FL = V[L, 2L, \ldots, -L, -2L, \ldots]$.

Next, we denote the deviation in the individual terrace width from the average by $\delta_n(t) = x_{n+1}(t) - x_n(t) - L$. Assuming small deviations, we expand Eq. (1) into a Taylor series up to terms linear in δ_n:

$$d\delta_n/dt = \sum_{m=\pm 1}^{\pm\infty} (\delta_{n+m} - \delta_n)\partial V/\partial r_m, \quad (2)$$

 © 2007 The American Physical Society

where the partial differentials $\partial V/\partial r_m$ are evaluated at $r_1 = L$, $r_2 = 2L, \ldots, r_{-1} = -L$, $r_{-2} = -2L$, and so on. Whether the step trains are stable upon the introduction of the linear perturbations can be determined by applying a standard capillary (sinusoidal) wave analysis [3,9], where the complex frequency $\Omega(K)$ of wave vector K, or, equivalently, the dispersion relation, is defined by the relation of $\partial\hat{\delta}/\partial t = \Omega(K)\hat{\delta}$ obtained by taking the Fourier transformation of Eq. (2), yielding:

$$\Omega(K) = \sum_{m=\pm 1}^{\pm\infty} [\exp(iKm) - 1]\partial V/\partial r_m. \tag{3}$$

Consequently, $\hat{\delta}$ evolves in time according to

$$\hat{\delta}(K, t) = \hat{\delta}(K, t_0)\exp[\Omega(K)(t - t_0)], \tag{4}$$

where $\hat{\delta}(K, t_0)$ is the Fourier component of the perturbation $\delta_n(t_0)$ at time t_0, and $\delta_n(t)$ can be obtained by taking the inverse Fourier transformation of Eq. (4). In general, $\Omega(K)$ is a complex number, whose imaginary part is given by the phase of $\hat{\delta}(K, t)/\hat{\delta}(K, t_0)$, which is also the rate of oscillation of the step deviation. The real part of $\Omega(K)$ is given as

$$\mathrm{Re}\,\Omega(K) = \frac{1}{t - t_0}\ln\left|\frac{\hat{\delta}(K, t)}{\hat{\delta}(K, t_0)}\right|, \tag{5}$$

which determines the rate of decay or amplification of the deviation. Based on Eq. (5), a dispersion relation can be determined if the step positions at only two subsequent times are measured. The real part of $\Omega(K)$ represents the growth rate of the Fourier component of the deviation with wave number K, $\hat{\delta}(K, t)$. A step flow is stable only when all of the Fourier components of the deviation decay, requiring $\Omega(K) < 0$ for all K.

Now we specify to the case of strained films, where the steps interact elastically. Following [3], the elastic driving force on the steps, defined as the energy reduction associated with the motion of step n, is

$$f_n = \sum_{m=\pm 1}^{\pm\infty}\left[\frac{\alpha_1}{x_{n+m} - x_n} - \frac{\alpha_2}{(x_{n+m} - x_n)^3}\right], \tag{6}$$

where $\alpha_1 = (2Y\varepsilon^2 h^4/\pi)(1 + \nu)/(1 - \nu)$, h is the step height, ε is the misfit strain between the overlayer and the substrate, Y is the Young's modulus, ν is Poisson's ratio, and α_2 depends on the magnitude of the force dipoles [3]. The two parameters $\alpha_1$and α_2 define a characteristic length scale $L_0 = \sqrt{\alpha_2/\alpha_1}$, characterizing the equilibrium separation between two steps isolated from all other steps. As usual, here we have neglected the interaction between adatoms and the steps [3,5,9,10]. The energy reduction given in Eq. (6) adds to the formation energy of adatoms on the terrace near step n. In equilibrium with step n, the coverage of adatoms is $c_{\mathrm{eq}}(x_n) = c_0\exp(-f_n A/k_B T)$, where $c_0 = \exp(-E_0/k_B T)$ is the equilibrium coverage in the absence of elastic interaction, with E_0 being the formation energy of an adatom on the terrace, A is the area a step advances upon reception of an adatom, k_B is the Boltzmann constant, and T is the substrate temperature. In the attachment-limited regime, the actual coverage of adatoms near a step, $c(x_n^{\pm})$ with the "$-$" and "$+$" signs indicating the upper and lower terraces, respectively, may defer from the equilibrium coverage $c_{\mathrm{eq}}(x_n)$. The difference drives the adatoms to attach to or detach from the step with the adatom attachment fluxes $-Ddc/dx = k_-[c(x_n^-) - c_{eq}(x_n)]$ at x_n^- and $-Ddc/dx = -k_+[c(x_n^+) - c_{eq}(x_n)]$ at x_n^+. Here D is the diffusion constant of adatoms on terraces, and $k_-$and k_+ are, respectively, the rate constants of attaching adatoms to a step from the upper and the lower terraces.

Using the attachment fluxes on steps as the boundary conditions to the diffusion equation on a terrace, we can solve for the steady-state adatom distribution $c(x)$, from which the velocity of step n can be obtained by calculating the net influx from both sides [3,5,9,10]:

$$\frac{dx_n}{dt} = \frac{-Q_{n-1} + Fl_{n-1}(\frac{1}{k_+} + \frac{l_{n-1}}{2D})}{\frac{1}{k_-} + \frac{1}{k_+} + \frac{l_{n-1}}{D}} + \frac{Q_n + Fl_n(\frac{1}{k_-} + \frac{l_n}{2D})}{\frac{1}{k_-} + \frac{1}{k_+} + \frac{l_n}{D}}, \tag{7}$$

where $l_n = x_{n+1} - x_n$ and $Q_n = c_{\mathrm{eq}}(x_{n+1}) - c_{\mathrm{eq}}(x_n)$.

Finally, the dispersion relation is obtained [9] from the linear stability analysis of Eq. (7):

$$\Omega(K) = \frac{1 - \cos(K)}{\frac{1}{k_-} + \frac{1}{k_+} + \frac{L}{D}}\left[\frac{\alpha_1 A c_0 S}{k_B T L^2} - F\frac{\frac{1}{(k_-)^2} - \frac{1}{(k_+)^2}}{\frac{1}{k_-} + \frac{1}{k_+} + \frac{L}{D}}\right] + iF\sin(K), \tag{8}$$

where $S = K(2\pi - K)[1 - \alpha_2/(4\alpha_1 L^2)K(2\pi - K)]$.

To test the validity of Eq. (8), we carry out numerical simulations of step evolution following the nonlinear equation of motion—Eq. (7). This exercise, in turn, also offers an opportunity to illustrate the power of Eq. (5). In our simulation, a unit cell containing 64 steps is periodically repeated, and the initial step positions are randomly assigned. The dimensionless parameters used for demonstration purposes are $\beta A c_0\alpha_1/L_0 = 0.02$, $FL^2/D = 0.1$, $D/(Lk_-) = 0.2$ for the unstable case and $\beta A c_0\alpha_1/L_0 = 0.02$, $FL^2/D = 1.0$, $D/(Lk_-) = 0.2$ for the stable case. In the unstable case [Fig. 1(a)], the steps bunch during time evolution, while, in the stable case [Fig. 1(b)], all of the steps flow parallel to each other as they evolve. Next, the ratio of the Fourier transforms of the step-width deviation $\delta(t)$ between two subsequent times is calculated for both cases, with the simulation results represented by the dashed lines and that from Eq. (8) by the solid lines [Figs. 1(c) and 1(d)]. In the plots, we choose $K = \pi/4$ as a representative component. Both cases exhibit oscillatory behavior, with

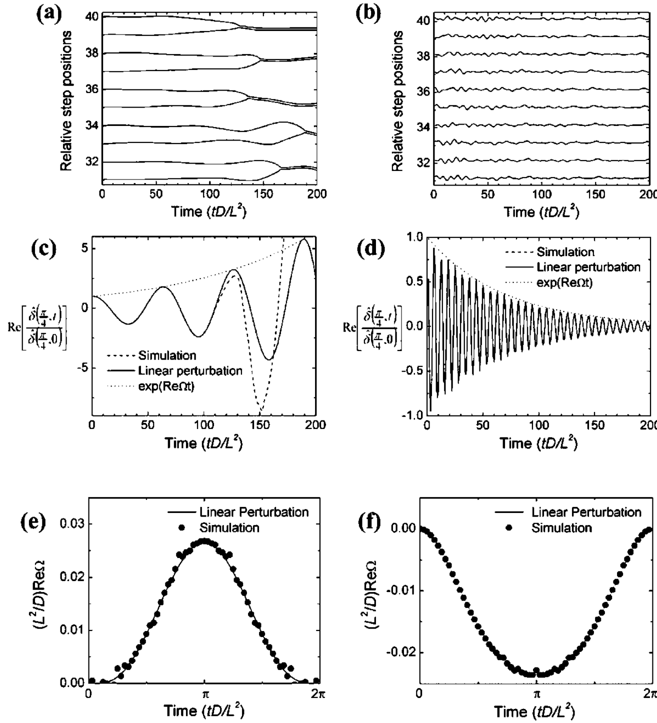

FIG. 1. Time evolution of the relative step positions in the (a) unstable and (b) stable regime. In (c) and (d), the dashed lines are from numerical simulations using Eq. (7), while the solid lines are based on linear stability analysis. The dynamics of the deviation amplitude increases exponentially in (c) the unstable case and decreases sinusoidally in (d) the stable case. The dispersion relations obtained from the numerical simulations using Eq. (7) and from linear stability analysis are compared in the (e) unstable and (f) stable cases.

the period given by the imaginary part of $\Omega(K)$. In Fig. 1(c), the amplitude increases exponentially, even though before bunching takes place the steps appear to preserve equidistance in Fig. 1(a), suggesting the existence of a critical film thickness in the bunching regime. In Fig. 1(d), the amplitude decays exponentially, indicative of persistent step flow. Also, a severe discrepancy appears only after step bunching in Fig. 1(c), where linear stability analysis is deemed to break down. In Figs. 1(e) and 1(f), the dispersion relation calculated from the simulation data, using Eq. (5), is compared to the result of linear stability analysis, Eq. (8). Excellent agreement is obtained for both cases; in particular, the unstable dynamics has a positive $\mathrm{Re}\Omega(K)$, whereas it is negative in the stable case.

Now we focus on the unstable case and determine the critical film thickness. Some simplifications based on physical considerations are introduced. First, adatoms on the lower terrace typically attach to a step much faster than adatoms on the upper terrace ($k_+ \ll k_-$, the Ehrlich-Schwoebel barrier effect [11]). Second, $L_0 \ll L$; therefore, the repulsion in Eq. (7) is negligible for the dynamics of nearly equidistant steps. Third, L is large enough that the system is in the diffusion-limited regime, with $k_- L/D \gg 1$. With these considerations, the real part of the dispersion relation (8) reduces to

$$\mathrm{Re}\,\Omega(K) \approx \frac{\alpha_1 A c_0 D}{k_B T L^3}\left[1 - \frac{L}{L^*}\frac{\pi^2}{K(2\pi - K)}\right](1 - \cos K), \tag{9}$$

which maximizes at $K = \pi$. Here $L^* = \pi^2 \alpha_1 A c_0 / k_B T D F$ is the critical terrace width above which a persistent step flow is the selected mode of growth. The maximum of Eq. (9) defines a time scale t_C, during which the fastest growing mode of the perturbation has developed large enough to cause step bunching. This time scale translates into a critical film thickness, via $\tau_C = F t_C$:

$$\frac{\tau_C}{F} \approx C \frac{k_B T L^3}{\alpha_1 A c_0 D}\left(1 - \frac{L}{L^*}\right)^{-1}. \tag{10}$$

The dimensionless parameter C is of order 1. The schematic behavior of τ_C as a function of L is shown in Fig. 2. If the terrace width is far below L^*, we have $\tau_C/F \sim L^3$. As L approaches L^*, τ_C increases rapidly towards infinity, signifying the persistent step-flow regime.

Here we note that, in the strongly unstable regime ($L \ll L^*$), once the vicinal angle or the average terrace width L is given, the rest of the right-hand side of Eq. (10) consists only of intrinsic or controllable growth parameters. This expression embodies several important messages. First, even if the growth conditions are chosen in the regime that step bunching is deemed to occur, there still exists a critical film thickness, below which growth proceeds via the step-flow mode, offering more opportunities to grow smooth films. Second, for a given system, the critical thickness scales with the deposition flux if other system and growth parameters are kept constant. Third, Eq. (10), in principle, offers an approach to determine some of the intrinsic energetic parameters of a system. We also note that Eq. (10) was derived within the linear stability analy-

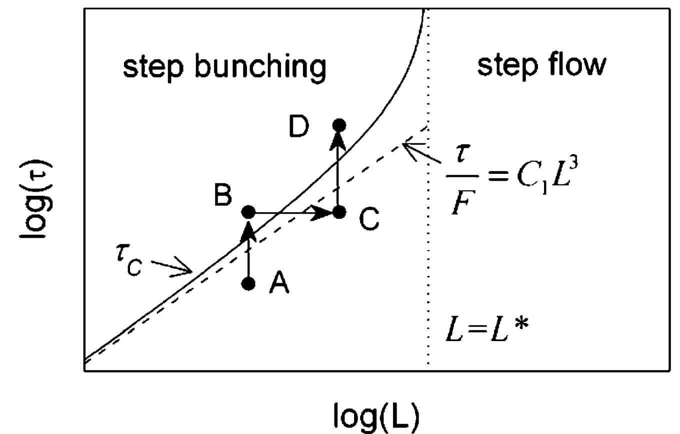

FIG. 2. A schematic view of the critical thickness τ_C as a function of the average terrace width L. When L is much shorter than L^*, τ_C scales with L^3. When L approaches L^*, τ_C deviates from $C_1 L^3$ and approaches infinity, with C_1 being a constant. The data points marked by the solid circles correspond to the AFM images shown in Fig. 3.

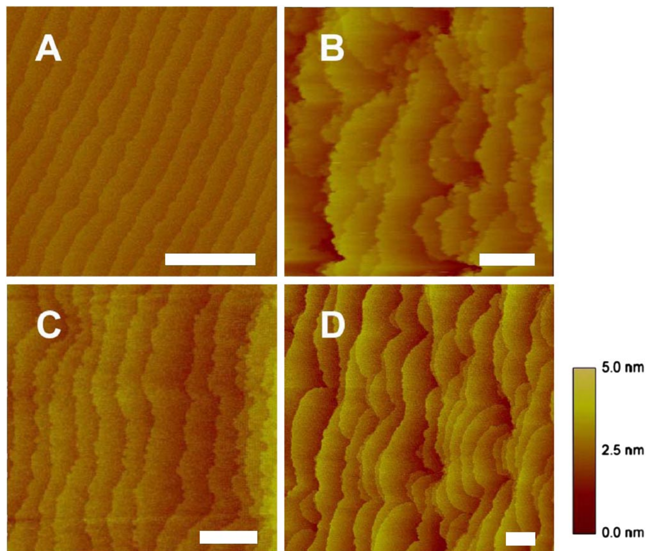

FIG. 3 (color online). AFM images of $SrRuO_3$ films of (a) 4 and (b) 10 nm grown on a vicinal $SrTiO_3$ substrate with a terrace width of ~200 nm. SRO films of (c) 10 and (d) 40 nm grown on a vicinal substrate with a terrace width of ~400 nm. The white scale bars are 10^3 nm in width.

sis, but its validity, in particular, in the strongly unstable regime where a simple L^3-scaling law is well defined, has been independently verified by numerical simulations of the step dynamics using the nonlinear equation of motion Eq. (7).

In principle, Eq. (10) can be applied to a wide range of heteroepitaxial growth systems. Nevertheless, a thorough literature review identified only limited indirect evidence [12], with no existing experimental or theoretical work directly addressing the dynamical transition from the step-flow growth regime below a certain critical film thickness to the step-bunching regime above. Here we present results of preliminary experimental studies of the SRO on STO growth system to check qualitatively the validity of Eq. (10). The results are presented in Fig. 3, showing the atomic force microscopy (AFM) images of SRO film morphologies at different film thicknesses on STO substrates of two different average terrace widths, under otherwise identical growth conditions by pulsed laser deposition [8]. The substrate temperature used was 700 °C, and the average deposition flux was $F = 0.06$ ML/s. X-ray diffraction confirmed that the SRO films were fully strained to match the STO substrates. Figures 3(a) and 3(b) were obtained on a substrate with $L \sim 200$ nm, but at different film thicknesses of 4 and 10 nm, respectively. Whereas the film illustrates step-flow growth at 4 nm [Fig. 3(a)], the growth mode is via step bunching when the film thickness is increased to 10 nm [Fig. 3(b)]. In contrast, when $L \sim 400$ nm, the growth mode is still via step flow at the film thickness of 10 nm [Fig. 3(c)]. Furthermore, when the film thickness is further increased to 40 nm on the wider terrace substrate, the growth mode again shows clear signs of step bunching [Fig. 3(d)]. These observations agree qualitatively with the predictions, as visualized in the schematic plots of Fig. 2, where the data points (A–D) correspond to the experimental images shown in Fig. 3 (see also Fig. 2 of Ref. [9], where images B and C were taken). In particular, the data clearly establish the existence of a critical film thickness before step bunching occurs.

Finally, we note that the steps shown in Fig. 3 are clearly meandered rather than straight, but as long as the magnitudes of the meandering are much smaller than the average terrace width, these steps can be modeled by 1D step trains. Such a condition holds as long as the system is still in the step-flow regime or when the bunching instability is just about to prevail. Also, the observed bunching occurred at a much lower thickness than what would be predicted by Eq. (10) if using the intrinsic parameters inferred previously [9]. The improved understanding achieved here necessitates a revisit of the earlier quantitative analysis, taking into consideration that an experimental observation of step flow (at a given film thickness) is not sufficient to delineate a region of *persistent* step flow. Such a more systematic experimental effort is in progress. The present work is expected to offer new pathways to obtain smooth films of desired thickness in other related systems where growth has to proceed in the strongly bunching regime.

This work was supported by DOE (Grant No. DE-FG02-03ER46091 and the Division of Materials Sciences and Engineering, Office of Basic Energy Sciences, under Contract No. DE-AC05-00OR22725 with ORNL, managed and operated by UT-Battelle, LLC).

[1] M. Kardar, G. Parisi, and Y.-C. Zhang, Phys. Rev. Lett. **56**, 889 (1986); V. A. Shchukin and D. Bimberg, Rev. Mod. Phys. **71**, 1125 (1999); J. Stangl, V. Holy , and G. Bauer, Rev. Mod. Phys. **76**, 725 (2004).
[2] C. S. Lent and P. I. Cohen, Surf. Sci. **139**, 121 (1984); C. Duport, P. Politi, and J. Villain, J. Phys. I **5**, 1317 (1995); O. Pierre-Louis *et al.*, Phys. Rev. Lett. **80**, 4221 (1998); G. H. Gilmer, H. C. Huang , and C. Roland , Comput. Mater. Sci. **12**, 354 (1998).
[3] J. Tersoff, Y. H. Phang, Z. Y. Zhang, and M. G. Lagally, Phys. Rev. Lett. **75**, 2730 (1995).
[4] O. Pierre-Louis, M. R. D'Orsogna, and T. L. Einstein, Phys. Rev. Lett. **82**, 3661 (1999); L. Bai, J. Tersoff, and F. Liu, Phys. Rev. Lett. **92**, 225503 (2004).
[5] Y. Xiang and W. E, Phys. Rev. B **69**, 035409 (2004).
[6] V. Popkov and J. Krug, Europhys. Lett. **72**, 1025 (2005).
[7] J. Choi *et al.*, Appl. Phys. Lett. **79**, 1447 (2001).
[8] H. N. Lee *et al.*, Appl. Phys. Lett. **84**, 4107 (2004); Nature (London) **433**, 395 (2005).
[9] W. Hong *et al.*, Phys. Rev. Lett. **95**, 095501 (2005).
[10] C. Duport, P. Nozieres, and J. Villain, Phys. Rev. Lett. **74**, 134 (1995).
[11] G. Ehrlich and F. G. Hudda, J. Chem. Phys. **44**, 1039 (1966); R. L. Schwoebel and E. J. Shipsey, J. Appl. Phys. **37**, 3682 (1966).
[12] R. Notzel, J. Temmyo, and T. Tamamura, Appl. Phys. Lett. **64**, 3557 (1994); F. Sanchez *et al.*, Phys. Rev. B **73**, 073401 (2006).